Title

MONTE CARLO CALCULATIONS OF NUCLEAR EVAPORATION PROCESSES IV. THE SPECTRA OF NEUTRONS AND CHARGED PARTICLES FROM NUCLEAR REACTIONS

Authors

Dostrovsiky, Israel
Fraenkel, Zeev
Winsberg, Lester.

Publication Date

1959-11-01

UCRL-8963

UNIVERSITY OF CALIFORNIA

Ernest O. Lawrence

Radiation Laboratory

BERKELEY, CALIFORNIA

DISCLAIMER

UCRL-8963

UNIVERSITY OF CALIFORNIA

Lawrence Radiation Laboratory
Berkeley, California

Contract No. W-7405-eng-48

MONTE CARLO CALCULATIONS OF NUCLEAR EVAPORATION PROCESSES
IV. THE SPECTRA OF NEUTRONS AND CHARGED PARTICLES FROM NUCLEAR REACTIONS

Israel Dostrovsky, Zeev Fraenkel, and Lester Winsberg

November 1959

Printed for the U.S. Atomic Energy Commission

MONTE CARLO CALCULATIONS OF NUCLEAR EVAPORATION PROCESSES

IV. THE SPECTRA OF NEUTRONS AND CHARGED PARTICLES FROM NUCLEAR REACTIONS* †

Israel Dostrovsky and Zeev Fraenkel
The Weizmann Institute of Science, Rehovoth, Israel

Lester Winsberg
Lawrence Radiation Laboratory, University of California
Berkeley, California
and
The Weizmann Institute of Science, Rehovoth, Israel

November 1959

ABSTRACT

The calculation of spectra of neutrons and charged particles and of cross sections for their production from nuclear reactions is compared with experimental values. A compound-nucleus mechanism followed by nuclear evaporation is assumed for the reactions Zr, Ta, Bi(14.1-Mev n,n'); Ni(13.4-17.5-Mev n,p); Cu, Pd(23-Mev p,α); and Ni(162-Mev O^{16},α). The production of neutrons and charged particles

---

*The preceding papers in this series are: Part I, "Systematics of Nuclear Evaporation," Dostrovsky, Bivins, and Rabinowitz, Phys. Rev. 111, 1659 (1958). Part II, "A Monte Carlo Calculation of Fission-Spallation Competition," Dostrovsky, Fraenkel, and Rabinowitz, "Proceedings of the Second International Conference on the Peaceful Uses of Atomic Energy," Geneva, 1958, 15, 301. Part III, "Applications to Low-Energy Reactions", Dostrovsky, Fraenkel, and Friedlander, submitted to Phys. Rev.

†Research performed in part under the auspices of the U.S. Atomic Energy commission.

from the interaction of 190-Mev protons with Ni, Ag, and Au is analyzed in terms of a nucleon cascade, followed by particle evaporation. The calculation of the nuclear evaporation is based on Weisskopf's statistical theory. Fairly good agreement is obtained for the values of the cross sections for producing these particles with an appropriate set of radius and level-density parameters in each case. There are serious discrepancies, however, in the comparison of the experimental and calculated spectra; many of the latter are deficient in low-energy neutrons and charged particles. Possible improvements in the calculation are discussed.

INTRODUCTION

Kinetic-energy spectra of particles emitted in nuclear reactions give valuable information on the mechanism of the reaction taking place. An angular distribution that is symmetric about 90° in the center-of-mass system is considered to be evidence for compound-nucleus formation.[1-3] At lower energies of excitation, isotropy in the center-of-mass system is taken to be evidence for such a process.[4-7] Comparison of the spectra with the statistical theory of Weisskopf provides a further check of the mechanism and, in addition, has been used to deduce the density of energy levels of excited nuclei. The results of various experiments, analyzed in this way, affirm the usefulness of the statistical approach but give conflicting values for the level density as a function of excitation energy and mass number.[5-9]

The comparison of the experimental results with the theory is fairly direct if the spectrum is that of the first evaporated particle only; however, it has been made for other cases as well.[10] In order to treat the complexities of the calculation more adequately when many particles are evaporated, a computer program has been prepared for the Weizmann Institute computer (WEIZAC). In Part I of this series,[11] spectra were calculated for particles from highly excited nuclei (100 to 700 Mev). The computer program was subsequently improved so as to make it applicable to lower energies of excitation.[12]

With the aid of this improved nuclear-evaporation calculation, it is possible to compute the spectra of particles that result from nuclei in any state of excitation. By these means we hope to further test the validity of the statistical theory and add more to what is known of level densities. Not

all of the pertinent experiments are considered here, since further changes in the computer program are suggested by recent experimental and theoretical developments and by the results of this paper. These suggested changes are discussed below.

An important criterion for the choice of a particular nuclear reaction A(x,y)B for this comparison is the absence or relative unimportance of non-compound-nucleus processes. The (α,p) and (p,α) reactions in the energy range 10 to 40 Mev are thought to fall into this category. The proton spectra from the bombardment of Cu, Ag, and Au with 40-Mev alpha particles have been measured by Eisberg, Igo, and Wegner and analyzed in terms of the statistical theory.[6] Unfortunately, the data were not presented in a form suitable for comparison here. The (p,α) reaction is considered below. Inelastic scattering and to a lesser extent (p,n) and (n,p) reactions are not well suited to this purpose. However, since no suitable experimental data were available on (α,n) reactions in the low energy range, the results of Ahn and Roberts[13] and of Rosen and Stewart[14] on the (n,n') reaction were used for the study of neutron spectra. The (n,p) reactions studied by Colli[15] et al. were used as an additional comparison for proton spectra.

Bombarding energies above 40 Mev lead to an increasing contribution of non-compound-nucleus processes if the bombarding particle is a nucleon or other light particle such as helium ions. With heavy ions as projectiles it is possible to form compound nuclei with excitation energies of more than 100 Mev (and with high angular momentum). So far only a few such studies are available. The recent determination by Knox, Quinton, and Anderson[3] of the alpha spectrum from the reaction of O^{16} ions on Ni is compared with our calculations in this work.

When the projectiles are light particles with energies of several hundred Mev, little or no compound-nucleus formation occurs. The projectile initiates a nucleon cascade which results in the emission of a few relatively energetic nucleons. The nuclei remaining at the end of the nucleon cascade have a distribution of values in A, Z, and excitation energy. The recent calculations of Metropolis et al.[16] have made such distributions available for a number of target nuclei throughout the periodic table and for proton bombarding energies up to 2 Bev. In this work we have used the results of Metropolis et al. for Cu, Ru, and Bi to compute the various spectra of particles emitted from the excited nuclei that result from the bombardment of Ni, Ag, and Au with protons of 190 Mev. The calculations were compared with the experimental results of Bailey[17] and of Gross.[18] Table I lists the reactions selected for comparison.

Table I

Reactions selected for comparison of calculated and experimental spectra and cross sections

Target	Projectile	Bombarding energy(lab) (Mev)	Emitted particle	Reference
Zr	n	14.1	n	13
Ta	n	14.1	n	14
Bi	n	14.1	n	14
Ni	n	13.4	p	15
Ni	n	14.1	p	23
Ni	n	17.5	p	15
Cu	p	23	α	24
Pd	p	23	α	24
Ni	O^{16}	162	α	3
Ni	p	190	n,p,d	17 and 18
Ag	p	190	T,He^3	17 and 18
Au	p	190	He^4	17 and 18

THE CALCULATIONS

The WEIZAC computer program for the Monte Carlo calculation of nuclear deexcitation has already been described in Parts I and III of this series.[11,12] The combinations of parameters used here are shown in Table II.

Table II

Parameters used in these calculations

Radius parameter, r_o (fermi)	Level density parameter, a (Mev^{-1})	Barrier correction (see text)
1.5	A/10	No
1.5	A/20	No
1.7	A/20	No
1.7	A/20	Yes

Calculations with a nuclear-radius parameter of 1.5 F (fermi) are described in detail in Part III.[12] Use of the radius parameter, 1.7 F, requires certain changes in the values of the coefficients used in calculating the inverse reaction cross sections, σ_c. The values that appear in the expression

$$\sigma_c/\sigma_g = \alpha(1 + \beta/\epsilon)$$

used for neutrons (cf. Eq. (2), Ref. 12) are $\alpha = 0.76 + 1.93A^{-1/3}$

$$\text{and} \quad \beta = \frac{1.66A^{-2/3} - 0.050}{0.76 + 1.93A^{-1/3}} \text{ Mev}, \qquad r_o = 1.7 \text{ F},$$

where σ_g is the geometric cross section.

For charged particles the inverse reaction cross section is given (cf. Eq. (3), Ref. 12) by

$$\sigma_c/\sigma_g = (1 + c_j) \cdot \left(1 - \frac{k_j v_j}{\epsilon}\right) ,$$

where the values of c_j and k_j are as given in Table III for $r_o = 1.7$ F (cf. Table II, Ref. 12). For protons, deuterons, and alpha particles, the constants c_j and k_j were chosen to give a good fit to the continuum-theory cross sections calculated by Shapiro[19] and Blatt and Weisskopf.[20] The relationship between the values of c and k for deterons, tritons, and He^3 and those for protons and alpha particles is assumed to be the same for $r_o = 1.7$ F as for 1.5 F.

Table III

Coefficients used in calculating the inverse reaction cross section of charged particles for $r_o = 1.7$ F

Z	k_p	c_p	k_α	c_α
20	0.51	0.00	0.81	0.0
30	0.60	-0.06	0.85	0.0
40	0.66	-0.10	0.89	0.0
50	0.68	-0.10	0.93[a]	0.0[a]

[a] Extrapolated values

Between 2000 and 10,000 evaporation cascades were computed for each reaction and set of parameters, so as to provide reasonable statistics. Except for the high-energy reactions the kinetic energy of the emitted particles was classed in 0.5-Mev intervals. In the high-energy reactions 1-Mev intervals were used.

COMPARISON WITH EXPERIMENTAL RESULTS

The comparison of the calculated and experimental particle spectra is given in Figs. 1-19.

Low-Energy Reactions

A. Neutrons from 14.1-Mev Neutron Bombardment

The space-integrated spectra obtained by Ahn and Roberts[13] are shown in Fig. 1, and those by Rosen and Stewart[14] in Figs. 2 and 3, together with the results of the Monte Carlo calculations. The calculated spectra were normalized so as to give the same total cross section for neutrons above 0.5-Mev kinetic energy. This procedure was adopted because no experimental data are available below that energy. Practically identical spectra are obtained for r_o = 1.5 F and r_o = 1.7 F. In Fig. 1 the maximum of the second neutron from Zr is at very low energy because the total kinetic energy available for two neutrons emitted is about 2.5 Mev. With the energy interval used in the calculations (0.5 Mev) the lower maximum is not resolved, and the net effect is the obliteration of the peak in the kinetic energy distribution. For Ta the total kinetic energy for both neutrons is about 6 Mev, for Bi about 9 Mev. The maximum kinetic energy of the second neutrons is therefore higher. The spectra show accordingly a single maximum at the average value of the nuclear "temperatures." The Zr spectrum seems to fit best with a value of a close to 10 Mev^{-1}. This value also gives a reasonable fit for the Bi spectrum. The Ta spectrum, however, requires a higher value of a. Several values, in addition to A/10 and A/20, were tried. The calculated spectrum that seems to fit the experimental data best is for a value of a of approximately 14 Mev^{-1}. It should

be remembered that both Bi^{209} and Zr^{90} have closed neutron shells, and a lower level density is to be expected. (This fact is taken into account in the calculation by subtracting a shell energy δ_s = 1.0 Mev from the residual excitation energy.[12] It seems however that this value of δ_s, which gives reasonable fit for the cross sections in the medium weight nuclei region ($24 \leq Z \leq 32$), does not give a large enough correction for heavier nuclei, such as Zr and Bi.) Because of the effect of the closed neutron shell, the results presented here do not permit a proper study of the A dependence of the level-density parameter. Further experiments with targets carefully chosen so as to be free from shell effects are clearly desirable.

A comparison of the calculated and experimental numbers of neutrons produced per inelastic collision for Zr, Ta, and Bi targets is shown in Table IV.

Table IV

Comparison of calculated and experimental numbers of neutrons produced per inelastic collision in the 14.1-Mev neutron bombardment of various elements

	Number of neutrons per inelastic collision			
	Calculated			Experimental
Target	r_o = 1.5 F, a = A/10	r_o = 1.5 F, a = A/20	r_o = 1.7 F, a = A/20	
Zr	1.62	1.51	1.48	1.62(ref.13)
Ta	2.00	1.99	1.99	1.90(ref.14)
Bi	2.00	2.00	2.00	1.96(ref.14)

B. Protons from 13.4-Mev and 17.5-Mev Neutron Bombardment

The proton kinetic-energy spectra for the Ni(n,p) reaction for two neutron energies, 13.4 Mev and 17.5 Mev, are shown in Figs. 4 and 5. The experimental points are those of Colli et al.[15] They were measured in the forward

direction (θ_{lab} = 0 to 35 deg). The calculated results were normalized so as to give the same total cross section of protons above 4 Mev as that given by Colli, since no data for lower kinetic energies are given by them.

The calculated spectra, especially for r_o = 1.5 F, are displaced toward higher energies with respect to the experimental results. (Figs. 4, 5). The calculated curves for r = 1.7 F, a = A/20 show clearly the contribution of protons from the (n,np) reaction. For this set of parameters at 13.4 Mev a small proportion of (n,np) reaction is calculated to be present (4%), but it is sufficient to affect the spectrum near threshold because of the low total energy available to the two emitted particles. For the 17.5-Mev neutrons (Fig. 5) the agreement between the calculated and experimental values seems to be much better. This results from the shifting of the maximum of the kinetic energy distribution to lower energies because of considerable proportions of second protons from the (n,np) reaction are present for all sets of parameters. (Only the high-energy part of the proton spectrum was measured experimentally, the low-energy part being below the experimental limit of 4 Mev. The calculated spectra are almost entirely above 4 Mev. Hence almost the total calculated spectrum has been normalized to what constitutes only the high-energy part of the experimental cross section. At the higher bombarding energy (Fig. 5) an appreciable part of both the experimental spectrum and the calculated spectrum is below the 4-Mev limit, hence the apparent differences in magnitude are much smaller.) Incidentally, this illustrates the care that is necessary in interpreting the dependence of the position of the maximum of kinetic energy on excitation energy. Ignoring the second proton in the example above could easily have led one to assume that the "temperature" of the compound nucleus actually decreased with increasing excitation energy!

Following Weisskopf,[21] the single-particle spectra of charged particles are given by the equation

$$P(\epsilon)d\epsilon = C\cdot\sigma_g\cdot\epsilon\left(1-\frac{V}{\epsilon}\right)\exp\left[2a^{1/2}(E-Q-\epsilon)^{1/2}\right], \qquad (1)$$

where $P(\epsilon)d\epsilon$ is the probability of emission of a particle with kinetic energy between ϵ and $\epsilon+d\epsilon$, C = a constant, V = the effective Coulomb barrier (corrected for penetration) = $k_j v_j$, $\underline{a}$ = the level-density parameter, E = the excitation energy of the nucleus, and Q = the separation energy for the emitted particle. A plot of $\log\frac{N(\epsilon)}{(\epsilon-V)}$ against $(E-Q-\epsilon)^{1/2}$ should lead to a straight line provided (a) the target is monoisotopic, (b) the particle under consideration is the only one or the first one to be emitted, and (c) a correct value of the effective Coulomb barrier is used. Here $N(\epsilon)$ is the number of experimentally measured protons per unit energy interval. Colli et al.[15] have plotted $\log\frac{N(\epsilon)}{\epsilon\,\sigma_c}$ against residual excitation energy $(E-Q-\epsilon)$. Since $\epsilon\cdot\sigma_c$ = const $(\epsilon - V)$, this plot is similar to the one described above, but, because the function $\log\frac{N(\epsilon)}{(\epsilon-V)}$ was plotted against the residual energy and not its square root, no straight-line portions are to be expected even in the region of single-particle emission. Furthermore, Colli et al. do not state the value of the Coulomb barrier (i.e. nuclear radius and penetrability) used by them to calculate σ_c. It is not clear, therefore, what degree of agreement between the curves for various energies one should expect.

In Figs. 6 and 7 we have replotted Colli's data against the square root of the residual excitation energy for two values of the nuclear-radius parameter and the corresponding penetrability. Also shown are our calculated spectra for a = A/20 drawn in the same way and with the same value of nuclear radius. Both calculated and experimental data were taken from Figs. 4 and 5 without any further

normalization. It is seen that here the agreement of the calculated and experimental points for r_o = 1.7 F is surprisingly good, especially for the 17.5-Mev data, and that a value of $\underline{a}$ = A/20 gives the correct slope. The agreement is good both in the straight-line regions representing essentially single particle emission and also in the part where the protons from (p,np) reactions are important. The discrepancy at very low residual energies (i.e. high proton kinetic energy) is undoubtedly due to direct interactions. It appears, therefore, that the validity of the statistical model is not challenged by Colli's results. It is unfortunate that data for protons below 4 Mev could not be obtained in this experiment, as it appears that in this range there are considerable discrepancies between calculations and experiment (see below). To make the comparison more valid the spectra were computed by taking into account the natural abundance of the various isotopes of nickel. From the fact that the fit of calculated and experimental data seems to be much better in Fig. 7 than it is in Figs. 4 and 5 it must be concluded that the direct comparison of calculated and experimental spectra (as shown in Figs. 4 and 5) permits a more rigorous test of the general validity of the statistical theory. It is for this reason that all other comparisons between calculated and experimental spectra discussed in this paper are presented in the form of the actual particle spectra rather than in the form of "level densities" (or log $\frac{N(\epsilon)}{\epsilon - V}$).

Colli et al.[15] do not give values for the total cross section for proton production. The calculated cross sections, using Bjorklund and Fernbach's value (1400 mb)[22] for the inelastic neutron cross section for Ni^{58}, agree well with the experimental values of Purser and Titterton[23] for the $Ni^{58}(n,p)Co^{58}$ and $Ni^{58}(n,np)Co^{57}$ reactions for r = 1.5 F, a = A/10 (see Table V). From Colli's

result one can obtain an approximate value for the partial cross section for protons above 4 Mev; these are 240 mb at 13.4 Mev and 380 mb at 17.5 Mev. It follows that a considerable proportion of the protons in Colli's experiment must have been below 4 Mev. However, the calculated spectra (Figs. 4 and 5) show very few protons below 4 Mev and are thus in disagreement with experiment.

C. Alpha Particles from 23-Mev Proton Bombardment

Calculated alpha spectra for the reaction Cu(p,α) and Pd(p,α) are shown in Figs. 8 and 9 together with the experimental values of Fulmer and Cohen[24] for an angle $\theta_{c.m.}$ = 150 deg. The calculated spectra of Figs. 8 and 9 were obtained by using Eq. (1) and not by the Monte Carlo calculation. This procedure was adopted because of the small cross section of alpha emission, which would have required undue computer time for satisfactory statistics by the Monte Carlo method. The procedure is justified only if all alpha's are emitted as first particles. Monte Carlo calculations showed that the ratio of cross sections (p,nα)/(p,α) is less than 0.005. The calculated curves were normalized to the differential (p,α) cross section at $\theta_{c.m.}$ = 150 deg as reported by Fulmer and Cohen.[24] In plotting the experimental results it was assumed that the differential cross section below 5 Mev is zero.

Table V

Comparison of experimental and calculated cross section for emission of protons and alpha particles

Reaction	Bombarding energy(lab) (Mev)	Ref.	Cross section, experimental (mb)	Cross section, calculated r_o = 1.5F a = A/10	r_o = 1.5F a = A/20	r_o = 1.7F a = A/20
$Ni^{58}(n,p)Co^{58}$	14.1	23	560 ± 110	655	651	595
$Ni^{58}(n,np)Co^{57}$	14.1	23	160 ± 40	141	90	362
$Cu(p,\alpha)Ni$	23	24	122 ± 25	23	76	160
$Pd(p,\alpha)Rh$	23	24	25 ± 5	1.3	6.5	47

Figure 8 indicates that the effective Coulomb barrier is much lower than that used in the calculation. A comparison of the slopes of the high-energy end of the spectra seems to indicate that the value of $\underline{a}$ = A/20 for the level-density parameter is the most suitable here. The Pd spectrum, Fig. 9, shows essentially no agreement with the calculation in either respect for the radius and level-density parameters used here. This lack of agreement is probably due in part to the increased proportion of various direct interactions. The differences between the results for Cu, for Pd, and for Au (where the discrepancy is even greater) can be understood when it is recalled that the cross section for emission of charged particles by evaporation decreases sharply with increasing Z. Therefore, on a relative basis, direct interactions become more prominent for higher values of Z.

In Table V are shown the calculated cross sections from emission from $Cu(p,\alpha)Ni$ and $Pd(p,\alpha)Rh$. It is obvious that r_o = 1.7 F is too large, since the experimental cross sections include the direct-interaction alpha particles and, therefore, should be higher than calculated values.

High-Energy Reactions

A. Alpha Particles from 162-Mev Oxygen-Ion Bombardment

The experimental results for the spectra of alpha particles emitted on the bombardment of Ni with 162-Mev O^{16} ions reported by Knox, Quinton, and Anderson[3], are shown in Fig. 10. The excitation energies of Kr compound nuclei lie in the range 123 to 136 Mev for the various isotopes. Alpha-emission spectra were calculated for the excited Kr nuclei in the proportions in which they are formed from the Ni isotopes and with the corresponding excitation energy. The calculated spectra were drawn normalized to the same area as the experimental results for 90 deg. This angle was chosen for comparison because it is the largest angle for which a complete spectrum was available, and in order to minimize the effects of direct interactions. The spectrum of $r_o = 1.7$ F and $\underline{a} = A/20$ seems to agree best with experiment, but even here the discrepancy in the Coulomb barrier is noticeable. Again the effective barrier is lower by several Mev than that used in the calculations.

B. Neutrons and Charged Particles from 190-Mev Proton Bombardment

Calculated spectra for neutrons, protons, deuterons, and alpha particles emitted from Ni, Ag, and Au bombarded with 190-Mev protons are compared in Figs. 11-19.

Since no prompt-cascade calculations are available for Ni and for Ag, use was made of the calculations available for Cu^{64} and Ru^{100}. In order to take into account the mass and charge difference between the Ru^{100} and Ag (nat) targets ($\Delta A = +7, +9$ and $\Delta Z = +3$), this difference was added to the mass and charge of each prompt-cascade result of the distribution before the evaporation calculation was started. The excitation energy of the prompt-cascade product

was not changed. Hence the distribution of prompt-cascade results with given A, Z, and E was substituted by A + ΔA, Z + ΔZ, E. In order to take into account the two natural isotopes Ag^{107} and Ag^{109} the calculations were repeated with different ΔA in the proportion of their natural abundance. The shifting procedure from Cu^{64} to Ni (nat) was similar. Although this procedure may not be completely reliable for the purpose of determining total-particle or product cross sections, the error introduced in the shape of the particle spectra is believed to be negligible. Since no prompt-cascade calculations are available for a bombarding energy of 190 Mev, the Ni and Ag spectra presented here were interpolated from the particle spectra calculated for bombarding energies of 156 Mev and 236 Mev. A comparison of the particle spectra for the two bombarding energies showed this interpolation to be entirely reliable.

In order to obtain the neutron spectrum from Au bombarded at 190 Mev, the prompt-cascade results for Bi^{209} were used after they had been shifted in the manner described. However, the bombarding energies nearest to 190 Mev for which calculations were available for this element are 82 Mev and 286 Mev. An interpolation over so wide an energy range was not thought to be reliable for neutrons or even possible for charged-particle spectra because of the scarcity of charged-particle evaporation from Au at a bombarding energy of 82 Mev. Hence the neutron spectrum was calculated for only one value of level-density parameter $\underline{a}$ and radius parameter r_o.

The calculated neutron spectra were normalized to the areas of the experimental spectra for 135 deg. The calculated charged-particle spectra were normalized to the experimental backward-hemisphere data. The experimental results are those of Bailey[17] and Gross.[18]

Again almost identical neutron spectra were obtained for r_o = 1.5 F and r_o = 1.7 F. This, together with the results of the low-excitation-energy region (Figs. 1-3) seems to indicate that the shape of the theoretical neutron spectra is roughly independent of the nuclear-radius parameter that was assumed in the calculation.

As seen in Figs. 11, 15, and 19, the calculated neutron spectra show a deficiency of low-energy particles, whereas both the shape and the absolute value of the high-energy part of the calculated neutron spectrum for a = A/10 show good agreement with the experimental results. The discrepancy in the low-energy neutrons was not improved appreciably when the calculations were repeated with a = A/6. As a result, the calculated differential cross sections are too low, as shown in Table VI. The experimental cross sections given in Table VI do not include prompt-cascade neutrons, according to Gross.[18]

The charged-particle spectra (Figs. 12, 13, 14, 16, 17 and 18) show the same effects as were already observed in the lower-energy region. In these cases the effective Coulomb barrier again seems to be lower than that used in the calculations. In Figs. 12 and 16, pertaining to proton spectra, the contribution of prompt-cascade protons is visible even in the backward hemisphere. This effect is far more evident in the forward direction. The deuteron spectra (Figs. 13 and 17) show also a contribution from prompt-cascade deuterons or--more likely--pickup by outgoing prompt-cascade nucleons.

The calculated cross sections for the emission of protons and alpha particles from Ni agree well with the experimental values in the backward direction particularly for a = A/20, Table VI. The agreement is less satisfactory for Ag. The calculated deuteron cross sections seem to be too high, especially in view of the contribution of nonevaporation deuterons to the

Table VI

Comparison of experimental and calculated cross sections (in mb/sterad) for the emission of neutrons, protons, deuterons, H^3, He^3, and He^4 upon the bombardment of Ni, Ag, and Au with 190-Mev protons

		n	p	d	t	He^3	He^4
Ni at 190 Mev							
Experimental[a]	Forward	109.5	120	9.25	2.06	1.93	17.4
	Backward		69	4.43	0.98	0.92	9.65
Prompt cascade (calculated)[b]		52.3	55				
r_o = 1.5 F $\underline{a}$ = A/10		65.9	90.5	6.57	0.70	0.92	5.75
r_o = 1.5 F $\underline{a}$ = A/20		51.6	76.5	11.2	1.72	2.16	10.0
r_o = 1.7 F $\underline{a}$ = A/20		45.7	80.6	11.5	1.87	2.62	13.95
r_o = 1.7 F $\underline{a}$ = A/20	(Corr)	36.1	81.8	12.85	1.93	3.95	26.0
Ag at 190 Mev							
Experimental[a]	Forward	412	128	13.7	4.53	1.76	23.2
	Backward		65.8	5.84	1.97	0.64	14.1
Prompt cascade (calculated)[b]		75	67				
r_o = 1.5 F $\underline{a}$ = A/10		394	49.05	8.69	1.52	0.28	9.07
r_o = 1.5 F $\underline{a}$ = A/20		321.5	46.2	17.6	6.18	1.18	17.67
r_o = 1.7 F $\underline{a}$ = A/20		320.8	42.05	18.0	5.62	0.997	20.25
r_o = 1.7 F $\underline{a}$ = A/20	(Corr)	255.7	53.4	22.5	6.87	3.02	58.35
Au at 190 Mev							
Experimental[a]	Forward	1085	136				15.0
	Backward		34				9.91
Prompt cascade (calculated)[b]		131	80				
r_o = 1.5 F $\underline{a}$ = A/10		980	12.31				2.40

[a] Results of L. E. Bailey[17] and E. Gross.[18] The experimental neutron cross sections do not include prompt-cascade neutrons, according to Gross.

[b] The value given here is that from Metropolis et al.[16] divided by 2π, since we assumed that the prompt nucleons go into the forward hemisphere.

experimental values. For deuterons, tritons, and He^3 particles $a = A/10$ seems to give better agreement with experimental cross sections. However, the statistics of the experimental and calculated values are rather poor in the last three cases.

DISCUSSION

In Part III of this series the excitation functions of various nuclear reactions are compared with the calculated values.[12] In general, the agreement is good. A similar comparison made here for the cross sections for production of light particles also indicates fairly good agreement, depending on the choice of radius and level-density parameters, Tables IV-VI. Especially striking is the comparison given in Table VI, since it is based on both a nucleon-cascade and an evaporation calculation. An agreement within a factor of two is indicated for most calculated entries in comparison with the experimental values for the backward hemisphere. In addition, the difference between the cross sections for formation of protons in the forward and backward hemispheres is in excellent agreement with the value of the cross section given by the cascade calculation, Table VI. It thus appears that the cross sections for formation of light particles are consistent with the two-stage model of nuclear reactions induced by high-energy protons, namely, a prompt cascade followed by an evaporation process. The treatment of the first stage, however, will have to be modified to account for the excess of heavier particles as well as of nucleons in the forward hemisphere.

The comparison of the spectra, on the other hand, indicates some serious discrepancies. The most striking feature of the calculated charged-particle

spectra is the apparent displacement of the curves toward higher energies with respect to the experimental results. This discrepancy cannot be reduced by any reasonable choice of level-density parameters. Although the barriers and their penetrability used in the calculation seem to need correction, this is not the sole difficulty, for the neutron spectra from the reactions induced by high-energy protons cannot be corrected in this way. This latter discrepancy is particularly serious, since it cannot possibly be explained by any of the direct-mechanism reactions postulated so far, nor can it be due to our incomplete knowledge of the Coulomb barrier. Moreover, no such discrepancy has been found in the lower energy region (Figs. 1-3). Changing the nuclear-radius parameter from 1.5 F to 1.7 F does indeed lead to a slight improvement in the spectra of charged particles, but this is still far from sufficient. This change has no effect on the neutron spectra. There may be two explanations, within the framework of the statistical model, why the calculated and observed spectra do not agree. In all our calculations we have assumed constant density of nuclear matter within the nucleus. The neglect of the diffuse edge of the nucleus may be expected to lead to errors in the computed inverse reaction cross sections. It is to be expected that both classical Coulomb barriers and their penetrability by charged particles will be affected.[25] The neutron cross sections may also be expected to be modified as a result of the change in the boundary conditions at the surface and the reduced reflection of the outgoing wave. Scott[26] and later Evans[27] have suggested that the effect of the diffuse edge on the Coulomb barrier may be approximated by using a larger effective nuclear radius. The choice of the larger nuclear-radius parameter (r_o = 1.7 F) may thus be regarded as a first approximation of the diffuse-edge effect. Igo has calculated the inverse-reaction cross section for alpha particles, based on a more correct representation

of the nuclear surface.[25] This would account for the emission of some lower-energy alpha particles, but is of insufficient magnitude to explain the large discrepancies noted in Figs. 8, 9, 10, 14, and 18. It is thus seen that the effect of the diffuse nuclear surface alone is insufficient to account for the discrepancies.

Another major correction may be necessary because the inverse-reaction cross section has to be calculated for the interaction of the outgoing particle and an excited nucleus. For charged-particle reactions such a dependence has already been postulated. Thus, Bagge concludes that the Coulomb barrier is reduced as a consequence of nuclear surface waves.[28] LeCouteur[29] and Fujimoto and Yamaguchi[30] have also assumed excitation-dependent barriers. More recently the need for such a correction was suggested by Fulmer and Cohen.[24] Dostrovsky, Bivins, and Rabinowitz[11] have illustrated the effect of such a correction on the yields and spectra of emitted particles. To investigate this point further we repeated some of our calculations, using excitation-dependent Coulomb barriers. The corrections used were of the form

$$V = kV_o \,/\, \left(1 + \sqrt{\frac{E_r}{2A}}\right), \qquad (2)$$

where V_o is the classical Coulomb barrier and E_r the residual excitation energy, and k is the penetration coefficient (Table III).

This particular form was chosen so as to give the same correction for Ag at 200 Mev excitation energy as that suggested by LeCouteur.[29]

At high excitation energies E_r can be taken, to a good approximation, as equal to the excitation energy prior to the emission of the particle. This makes it possible to use the same computer program with only minor changes. At

lower energies and towards the end of the high-energy evaporation cascade this assumption is not valid. The proper procedure would be to compute the inverse reaction cross section for each choice of kinetic energy of the outgoing particles. To do this properly requires an entirely new program, and in view of the tentative and doubtful nature of the correction, no attempt has been made to compose such a program. As is seen in Figs. 10, 12, 13, 14, 16, 17 and 18, the barrier correction of Eq. (2) does indeed lead to a much better agreement with experimental spectra, and even better agreement might possibly be obtained with other values of r_o and $\underline{a}$. However, the cross sections for the emission of deuterons, tritons, He^3, and He^4 particles are far too high with this correction, while that for the neutrons is too low (Table VI). It should be remembered that by use of Eq. (2) only the emission of charged particles is corrected, while that of the neutrons remains unchanged. This is evidently unsatisfactory, and a more rigorous treatment should also attempt to describe the dependence of the neutron-capture cross section on the excitation energy of the target nucleus. The unfavorable effect of the correction on the ratio of protons to alpha particles emitted also indicates that its form is unsatisfactory.

The same correction was applied also to the calculation of the alpha-particle spectra from the bombardment of natural Ni with 162-Mev O^{16} ions, (Fig. 10). Here it seems to be somewhat too powerful, indicating that the form chosen was not quite correct. However, no attempts were made to find better forms of this correction.

Clearly an excitation-energy-dependent Coulomb barrier, as suggested by Fulmer and Cohen[24] and others, will not in itself lead to a satisfactory agreement between calculated and experimental spectra and particle cross sections.

A more rigorous treatment of inverse-reaction cross sections, taking into account both the diffuse edge of the nucleus and its excitation, is highly desirable. Only then will it be possible to examine more quantitatively the validity of the statistical model.

ACKNOWLEDGMENTS

During the course of this work, one of the authors (L.W.) was a guest at the Weizmann Institute of Science. He is deeply grateful for the cordiality extended to him. We wish to thank the authors named in Reference 16 for giving us the results of their calculations. The assistance of Mrs. Miriam Berko in tabulating the data and preparing the figures is gratefully acknowledged.

REFERENCES

1. L. Wolfenstein, Phys. Rev. 82, 690 (1951).
2. T. Ericson and V. Strutinski, Nuclear Phys. 8, 284 (1958).
3. Knox, Quinton, and Anderson, Phys. Rev. Letters 2, 402 (1959).
4. W. Hauser and H. Feshbach, Phys. Rev. 87, 366 (1952).
5. P. C. Gugelot, Phys. Rev. 93, 425 (1954).
6. Eisberg, Igo, and Wegner, Phys. Rev. 100, 1309 (1955).
7. G. Igo, Phys. Rev. 106, 256 (1957).
8. G. Igo and H. E. Wegner, Phys. Rev. 102, 1364 (1956).
9. D. L. Allan, Nuclear Phys. 10, 348 (1959).
10. J. M. B. Lang and K. J. LeCouteur, Proc. Phys. Soc. (London) A67, 586 (1954).
11. Dostrovsky, Bivins, and Rabinowitz, Phys. Rev. 111, 1659 (1958).
12. Dostrovsky, Fraenkel, and Friedlander, submitted to Phys. Rev.
13. S. E. Ahn and J. H. Roberts, Phys. Rev. 108, 110 (1957).
14. L. Rosen and L. Stewart, Phys. Rev. 107, 824 (1957).
15. Colli, Pignanelli, Rytz, and Zurmühle, Nuovo cimento 9, 280 (1958).
16. Metropolis, Bivins, Storm, Turkevich, Miller, and Friedlander, Phys. Rev. 110, 185 (1958); Metropolis, Bivins, Storm, Miller, Friedlander, and Turkevich, Phys. Rev. 110, 204 (1958).
17. L. Evan Bailey, Angle and Energy Distributions of Charged Particles from the High-Energy Nuclear Bombardment of Various Elements (Thesis), University of California Radiation Laboratory, Report UCRL-3334, March 1956 (unpublished).
18. Edward Gross, The Absolute Yield of Low-Energy Neutrons from 190-Mev Proton Bombardment of Gold, Silver, Nickel, Aluminum and Carbon (Thesis), University of California Radiation Laboratory Report, UCRL-3330, Feb. 1956 (unpublished).

19. M. M. Shapiro, Phys. Rev. 90, 171 (1953).

20. J. Blatt and V. F. Weisskopf, Theoretical Nuclear Physics (John Wiley and Sons, New York, 1952).

21. V. Weisskopf, Phys. Rev. 52, 295 (1937).

22. F. Bjorklund and S. Fernbach, Phys. Rev. 109, 1295 (1958).

23. K. H. Purser and E. W. Titterton, The $Ni^{58}(n,p)Co^{58}$, $Ni^{58}(n,2n)Ni^{57}$, $Ni^{58}(n,np)Co^{57}$ Cross Sections at 15.1 Mev, Australian National University Report ANU/P-200, Nov. 1958.

24. C. B. Fulmer and B. L. Cohen, Phys. Rev. 112, 1672 (1958).

25. G. Igo, Phys. Rev. (to be published).

26. J. M. C. Scott, Phil. Mag., Ser. 7, 45, 441 (1954).

27. J. A. Evans, Proc. Phys. Soc. (London) 73, 33 (1959).

28. E. Bagge, Ann. Physik 33, 389 (1938).

29. K. J. LeCouteur, Proc. Phys. Soc. (London) A63, 259 (1950).

30. Y. Fujimoto and Y. Yamaguchi, Progr. Theoret. Phys. (Japan) 5, 76 (1950).

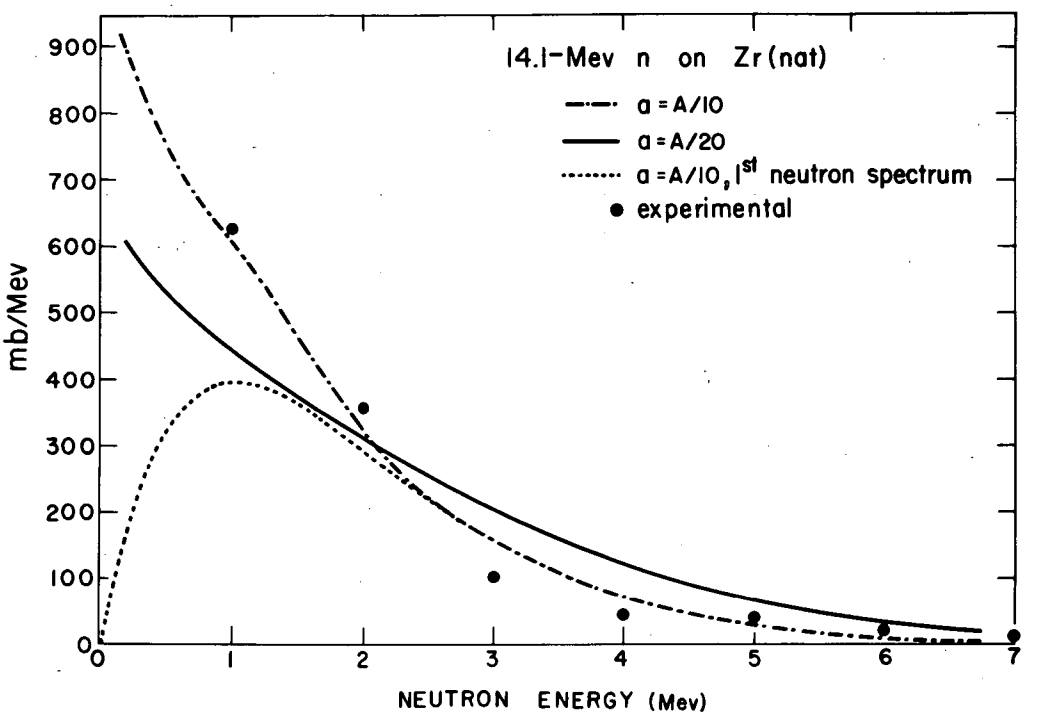

MU-18585

Fig. 1. Comparison of calculated spectra of neutrons from Zr (nat) bombarded with 14.1-Mev neutrons with the experimental results of Ahn and Roberts.[13]

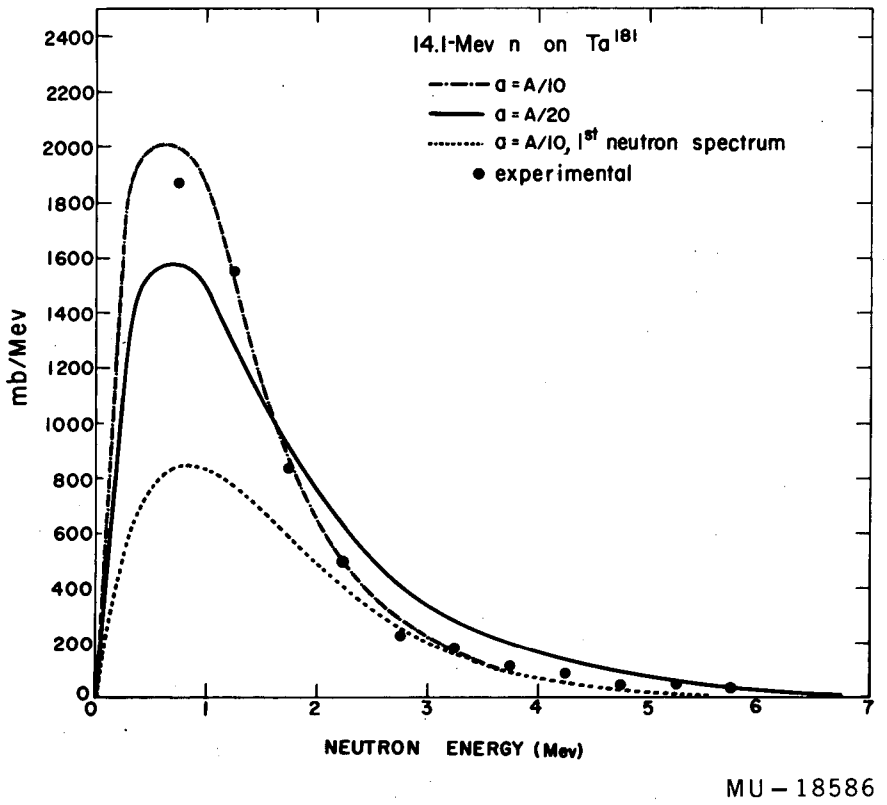

Fig. 2. Comparison of calculated spectra of neutrons from Ta^{181} bombarded with 14.1-Mev neutrons with the experimental values of Rosen and Stewart.[14]

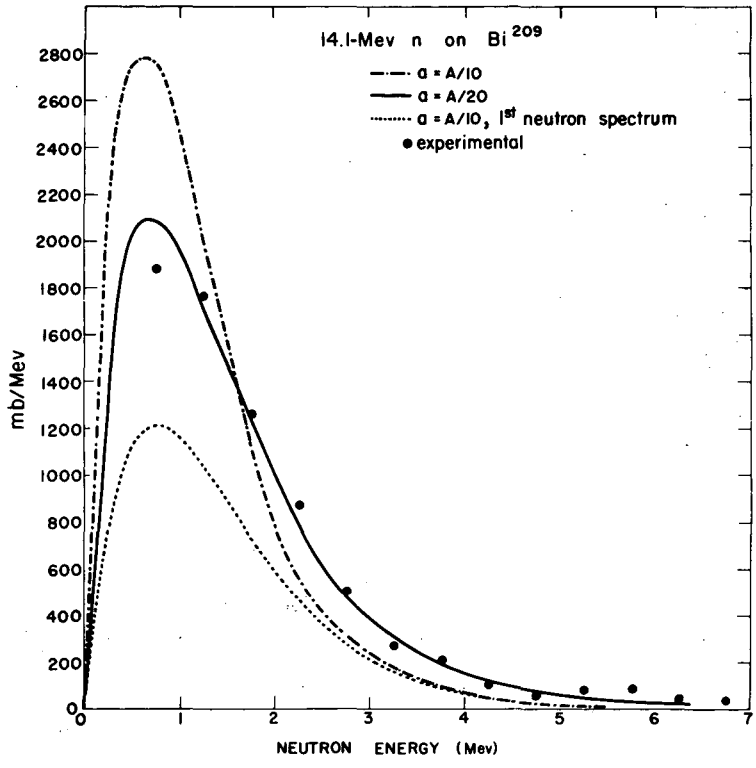

MU-18587

Fig. 3. Comparison of calculated spectra of neutrons from Bi^{209} bombarded with 14.1-Mev neutrons with the experimental values of Rosen and Stewart.[14]

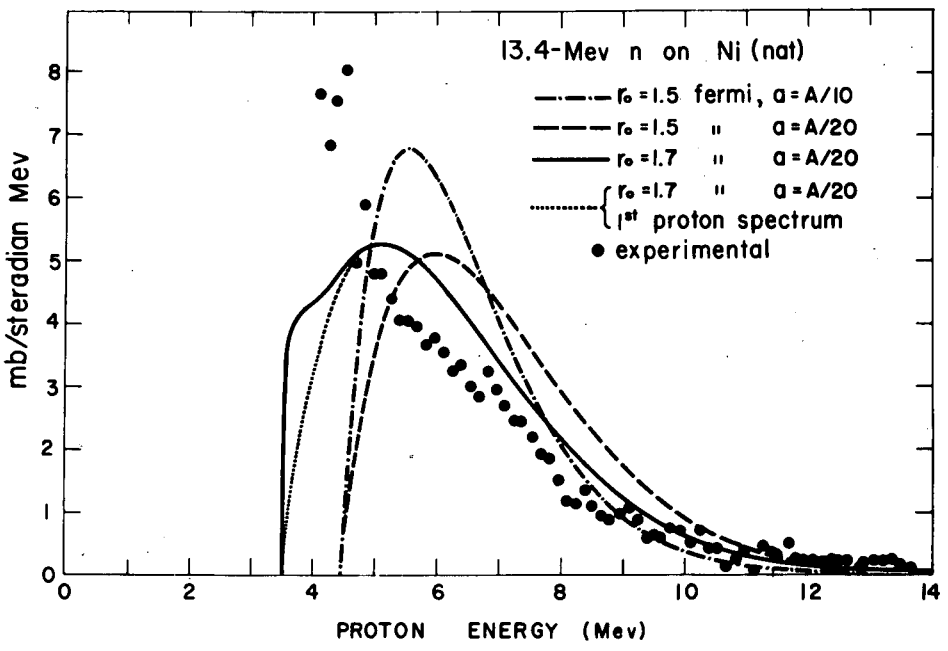

MU-18588

Fig. 4. Comparison of calculated spectra of protons emitted from Ni (nat) bombarded with 13.4-Mev neutrons with the experimental results of Colli et al.[15]

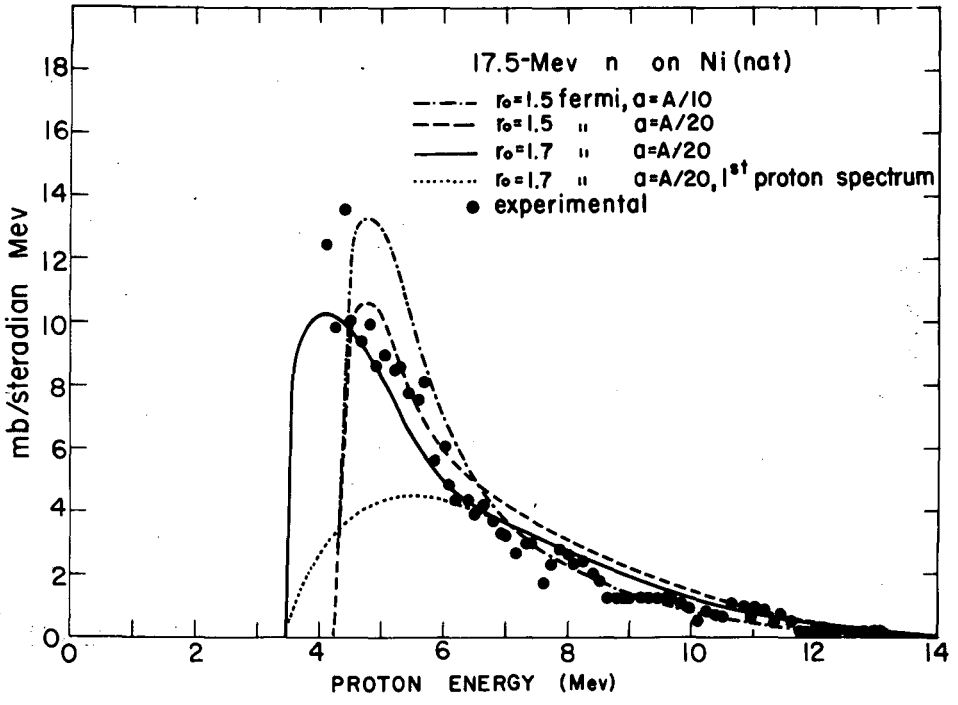

MU-18589

Fig. 5. Comparison of calculated spectra of protons emitted from Ni (nat) bombarded with 17.5-Mev neutrons with the experimental results of Colli et al.[15]

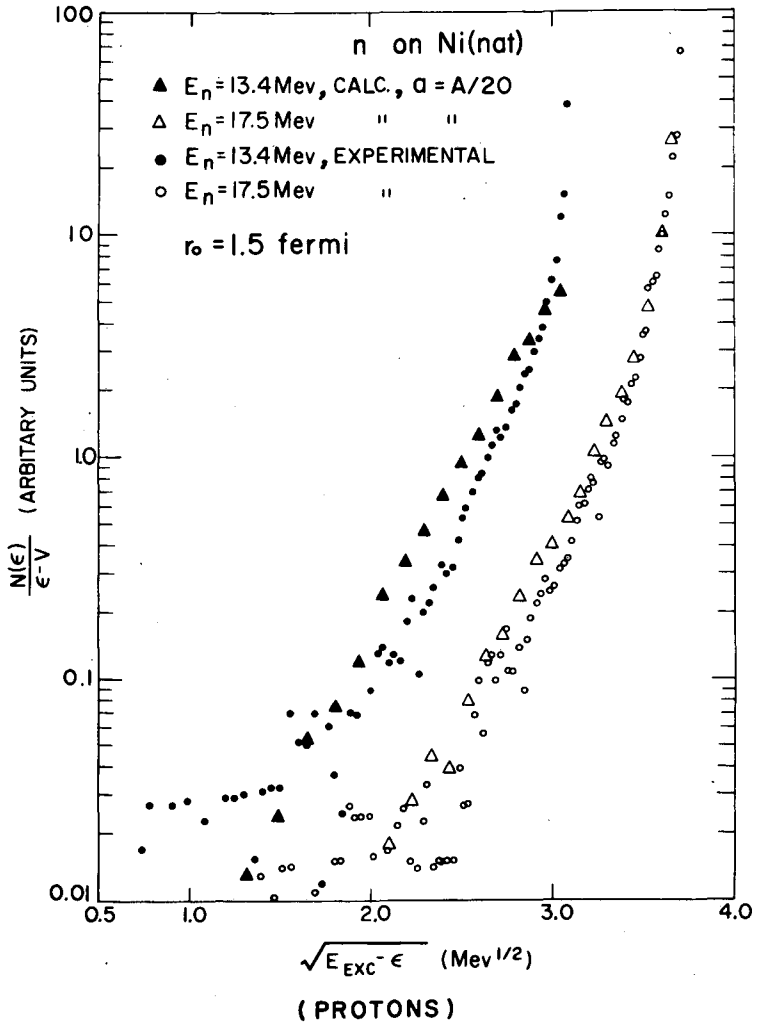

Fig. 6. $N(\epsilon)/(\epsilon - V)$ vs. the square root of the residual excitation energy as obtained from Figs. 4 and 5 for a nuclear radius parameter of r_o = 1.5 F and a level-density parameter of a = A/20.

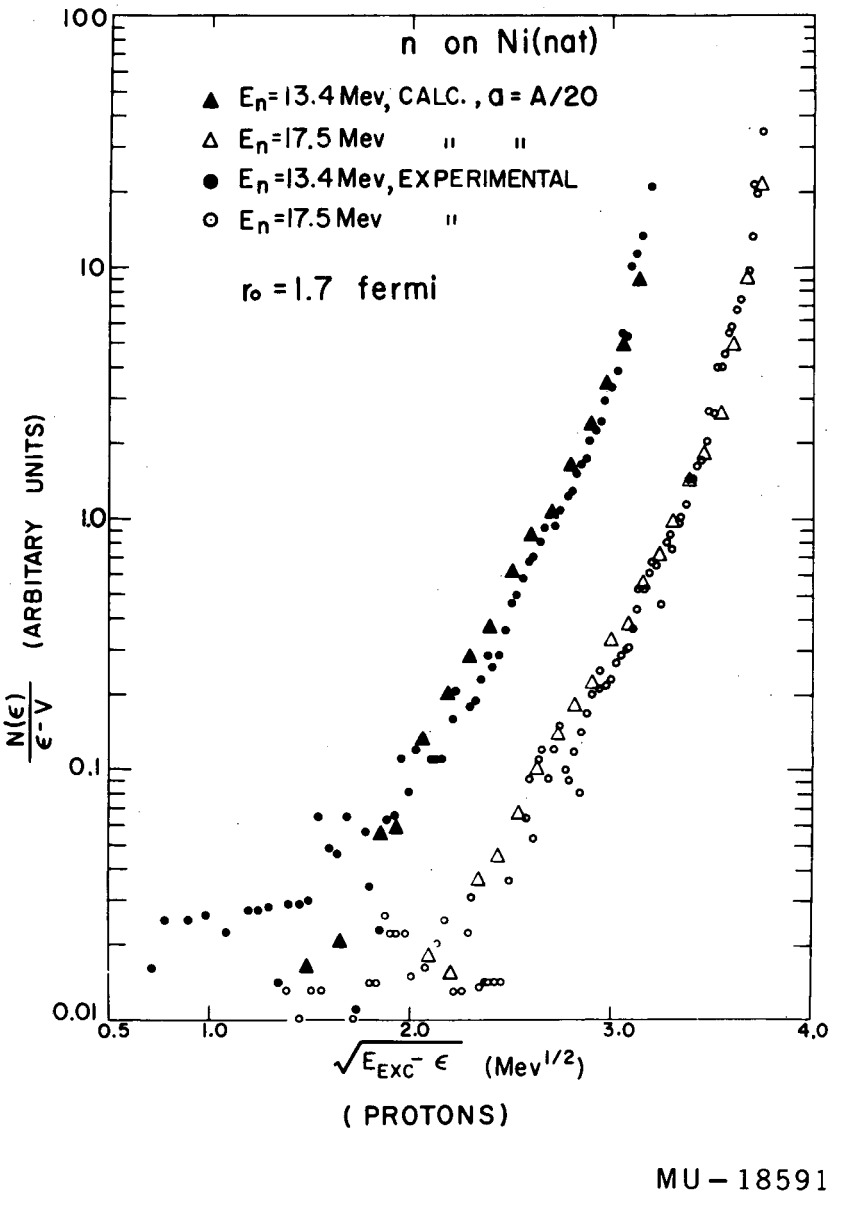

Fig. 7. $N(\epsilon)/(\epsilon - V)$ vs. the square root of the residual excitation energy as obtained from Figs. 4 and 5 for a nuclear radius parameter of r_o = 1.7 F and a level-density parameter of a = A/20.

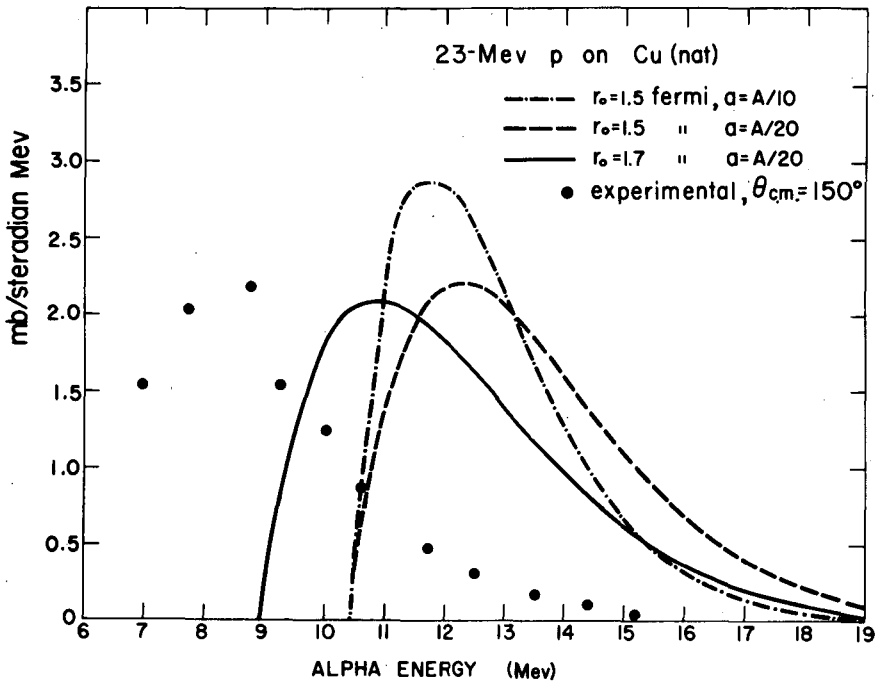

MU-18592

Fig. 8. Comparison of calculated spectra of alpha particles from Cu (nat) bombarded with 23-Mev protons with the experimental results of Fulmer and Cohen[24] for $\theta_{c.m.}$ = 150 deg.

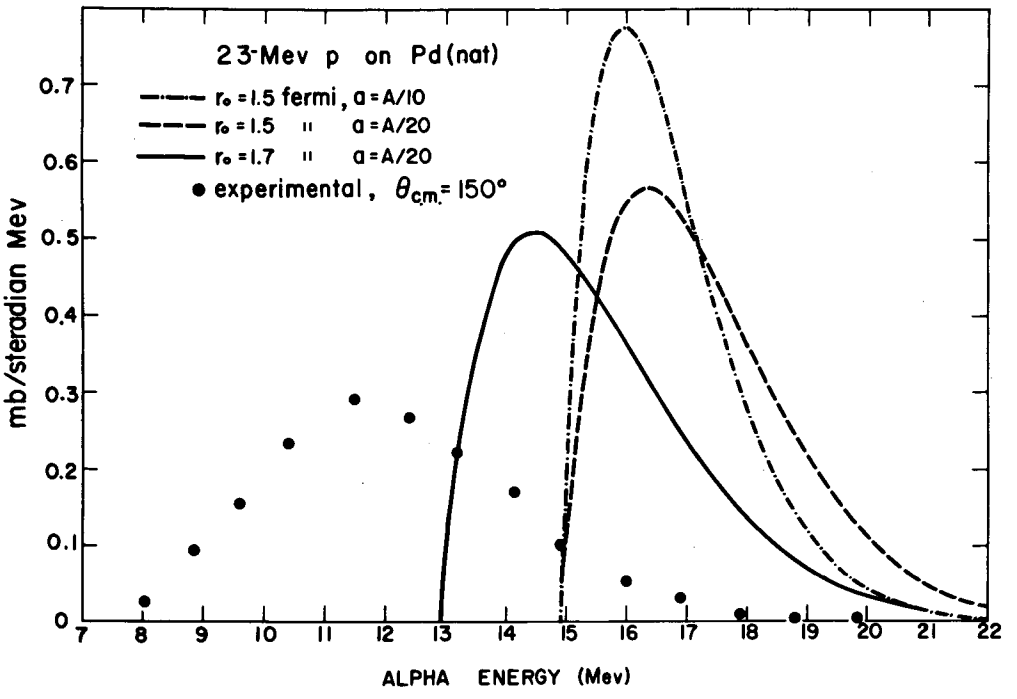

MU-18593

Fig. 9. Comparison of calculated spectra of alpha particles from Pd (nat) bombarded with 23-Mev protons with the experimental results of Fulmer and Cohen[24] for $\theta_{c.m.}$ = 150 deg.

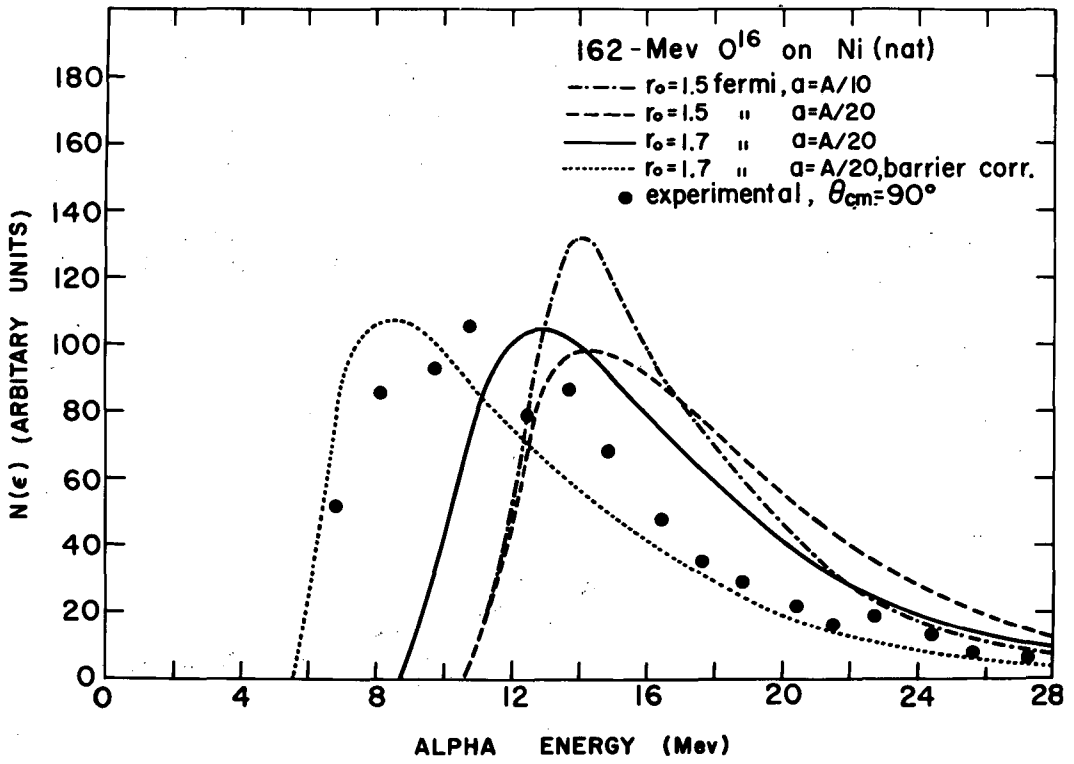

Fig. 10. Comparison of calculated spectra of alpha particles from Ni (nat) bombarded with 162-Mev O^{16} ions with the experimental results of Knox, Anderson, and Quinton[3] for $\theta_{c.m.}$ = 90 deg. For details of the barrier correction see Discussion.

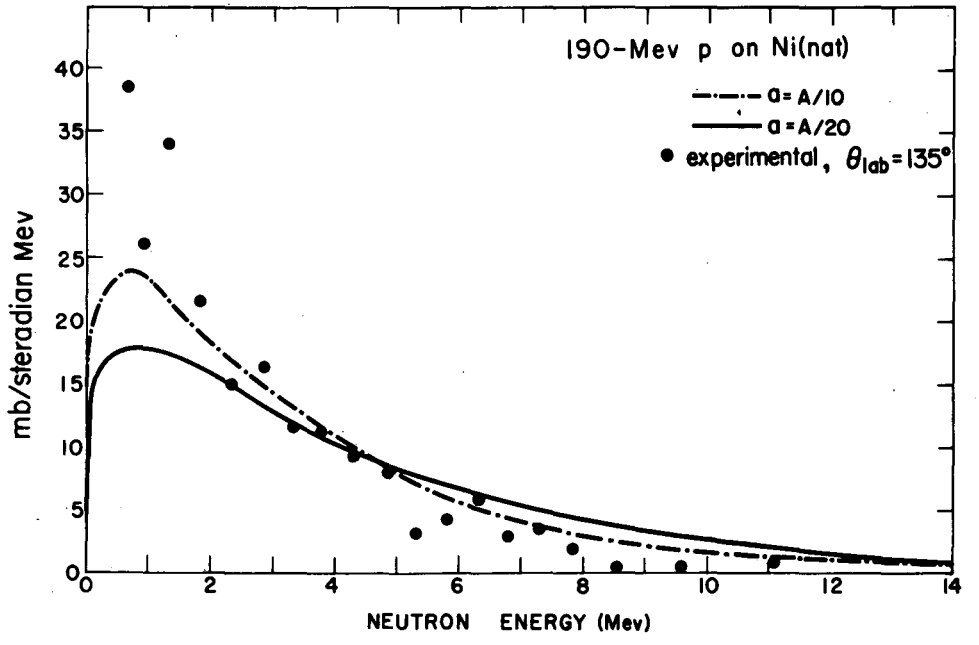

MU-18595

Fig. 11. Comparison of calculated evaporation spectra of neutrons from Ni (nat) bombarded with 190-Mev protons with the results of Gross[18] for θ_{lab} = 135 deg.

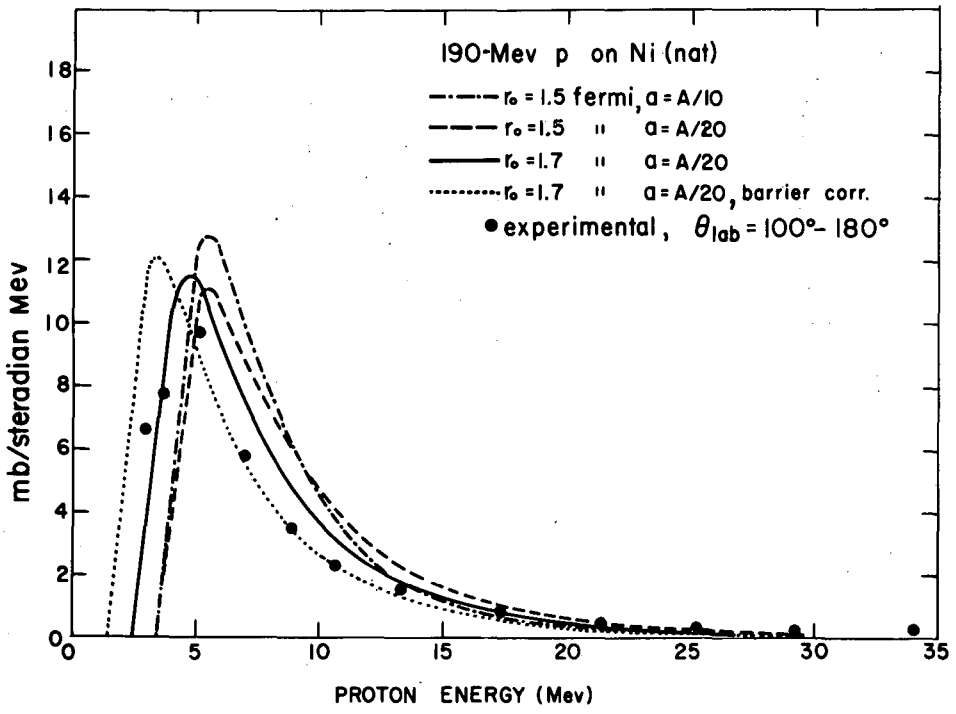

MU – 18596

Fig. 12. Comparison of calculated evaporation spectra of protons from Ni (nat) bombarded with 190-Mev protons with the results of Bailey[17] for θ_{lab} = 100 to 180 deg. For details of the barrier correction see Discussion.

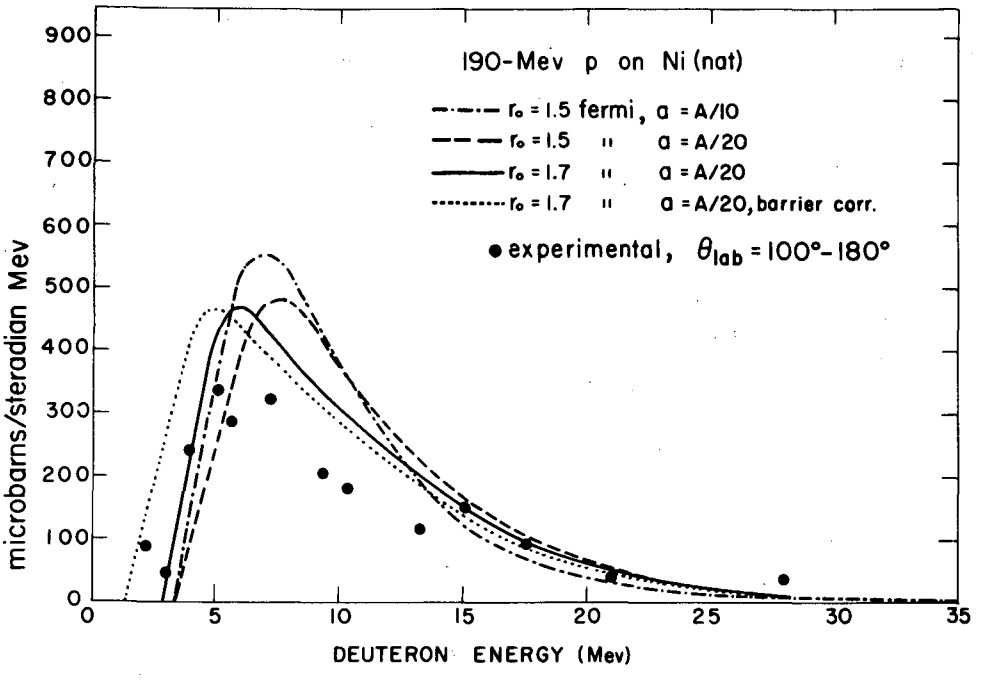

MU – 18597

Fig. 13. Comparison of calculated evaporation spectra of deuterons from Ni (nat) bombarded with 190-Mev protons with the results of Bailey[17] for θ_{lab} = 100 to 180 deg. For details of the barrier correction see Discussion.

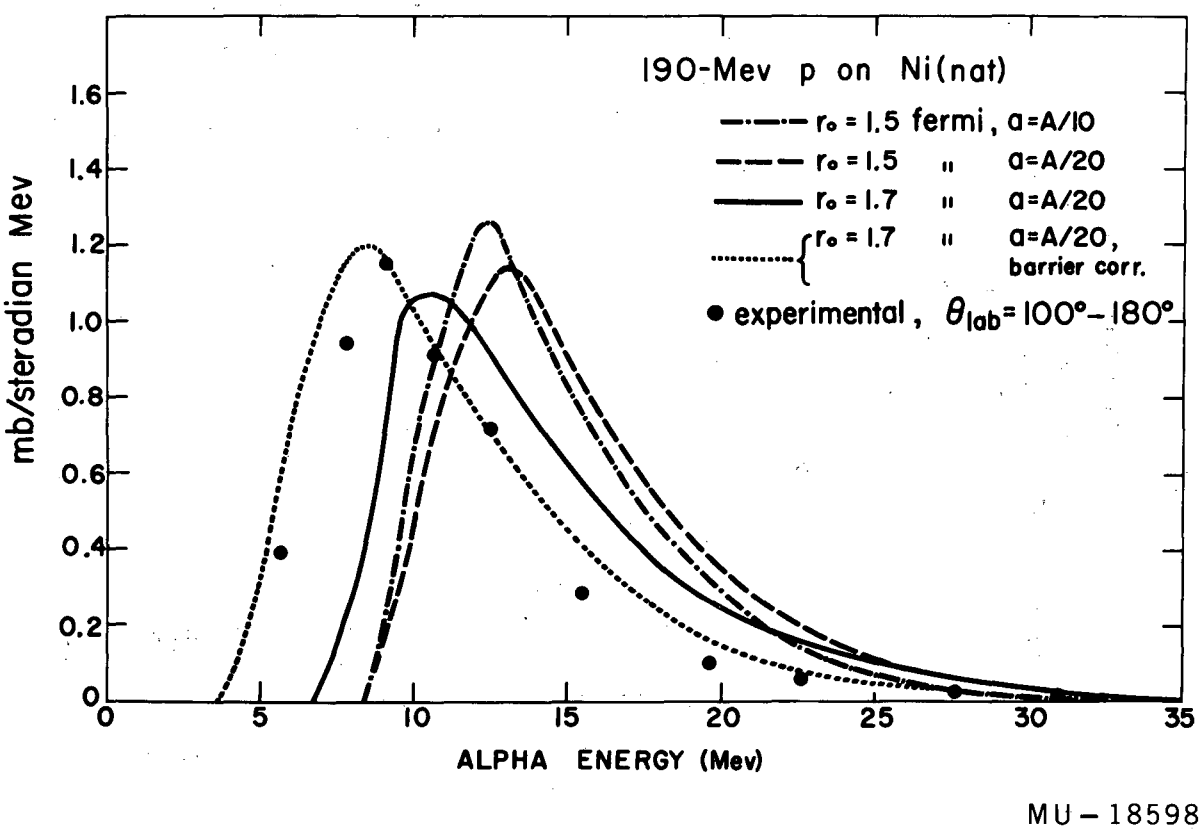

Fig. 14. Comparison of calculated evaporation spectra of alpha particles from Ni (nat) bombarded with 190-Mev protons with the results of Bailey[17] for θ_{lab} = 100 to 180 deg. For details of the barrier correction see Discussion.

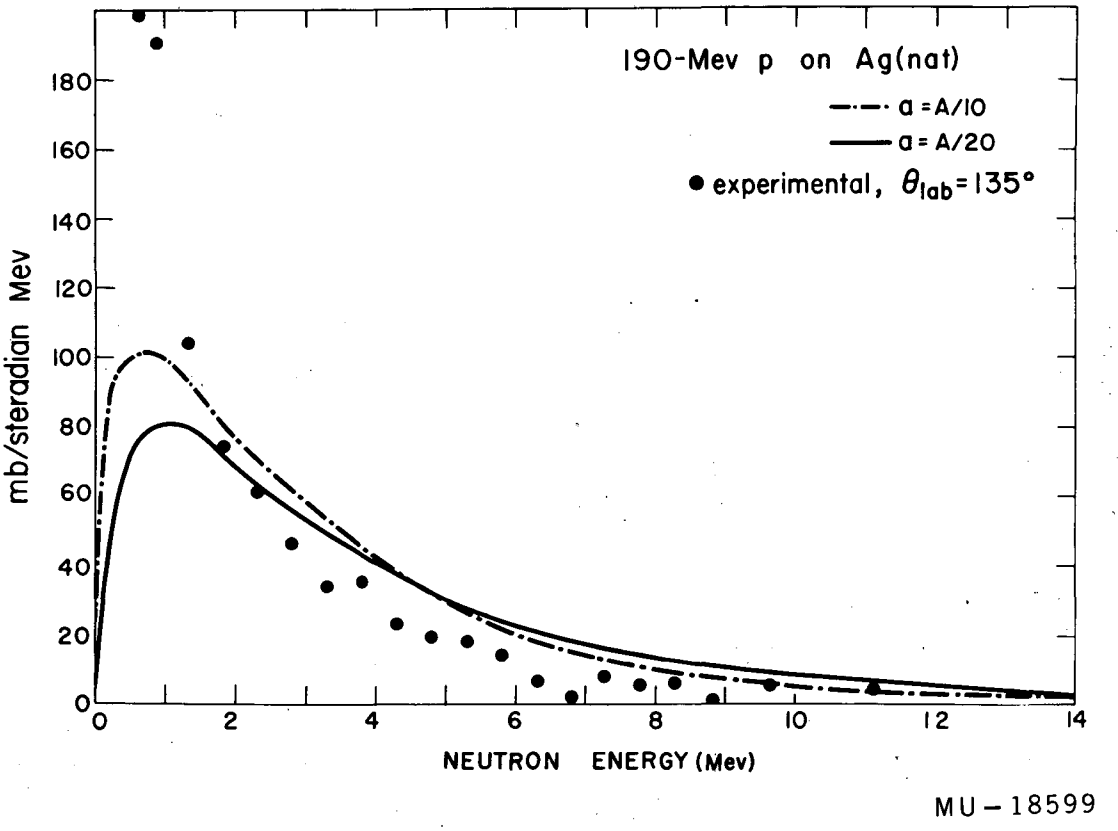

Fig. 15. Comparison of calculated evaporation spectra of neutrons from Ag (nat) bombarded with 190-Mev protons with the results of Gross[18] for θ_{lab} = 135 deg.

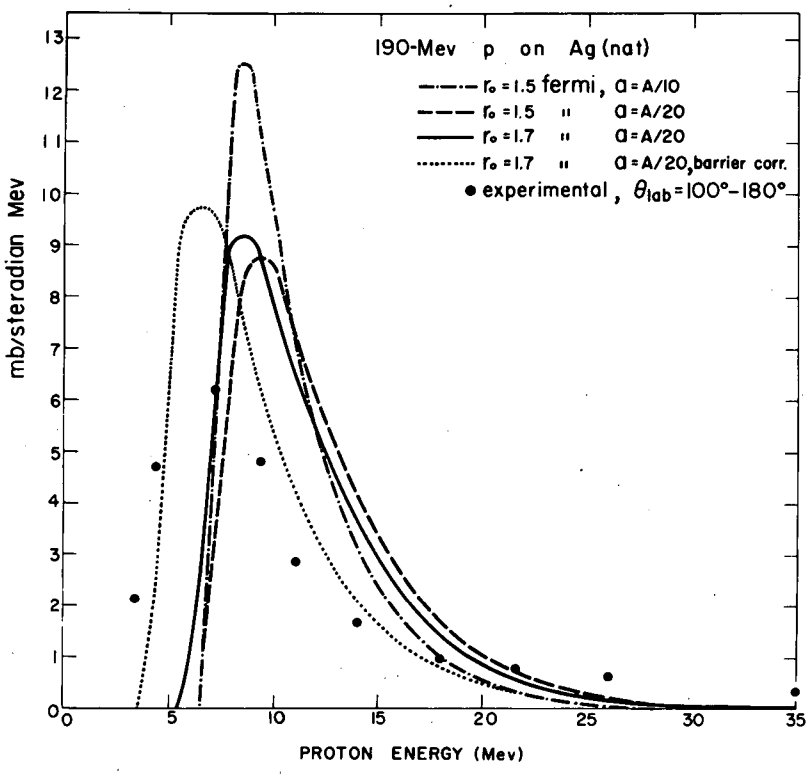

MU-18600

Fig. 16. Comparison of calculated evaporation spectra of protons from Ag (nat) bombarded with 190-Mev protons with the results of Bailey[17] for θ_{lab} = 100 to 180 deg. For details of the barrier correction see Discussion.

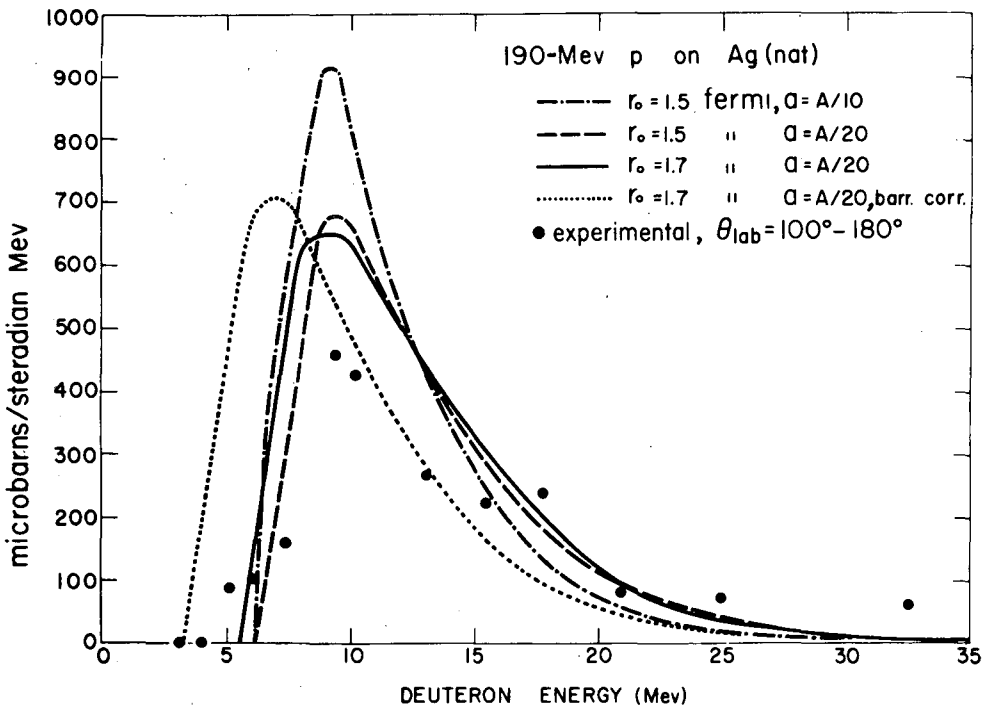

MU - 18601

Fig. 17. Comparison of calculated evaporation spectra of deuterons from Ag (nat) bombarded with 190-Mev protons with the results of Bailey[17] for θ_{lab} = 100 to 180 deg. For details of the barrier correction see Discussion.

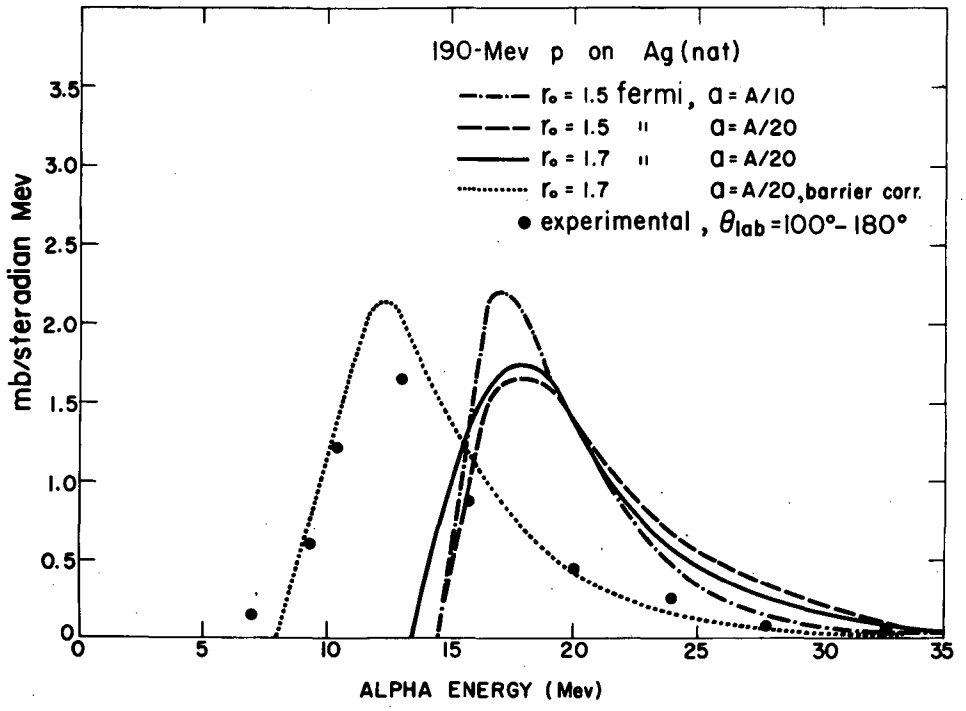

MU-18602

Fig. 18. Comparison of calculated evaporation spectra of alpha particles from Ag (nat) bombarded with 190-Mev protons with the results of Bailey[17] for θ_{lab} = 100 to 180 deg. For details of the barrier correction see Discussion.

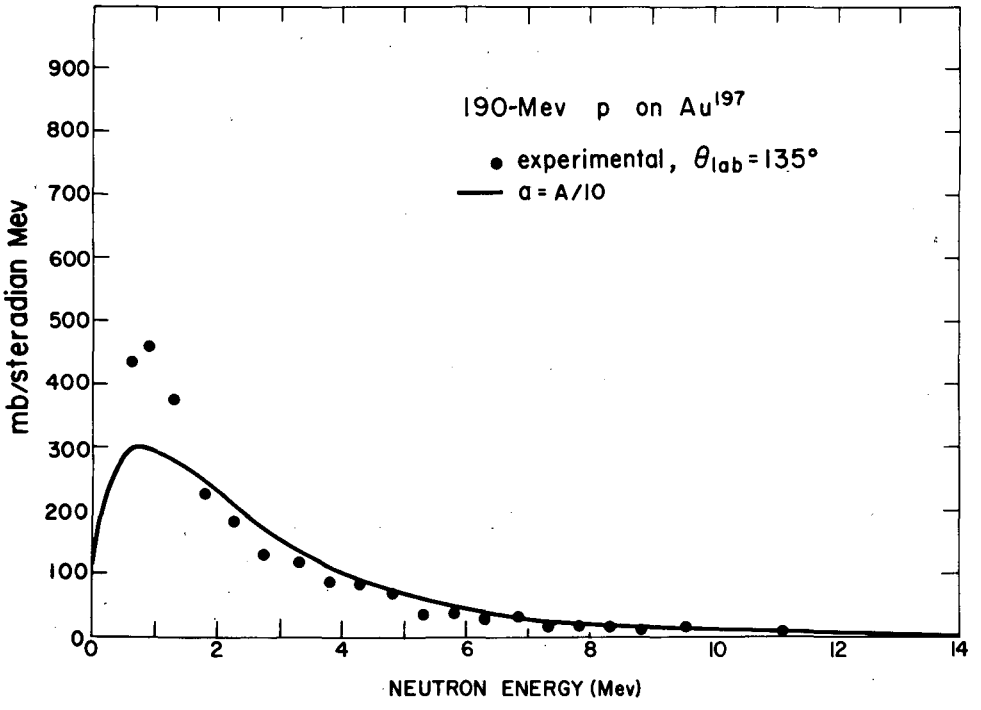

MU-18603

Fig. 19. Comparison of calculated evaporation spectra of neutrons from Au^{197} bombarded with 190-Mev protons with the results of Gross[18] for θ_{lab} = 135 deg.